SUPPLEMENTARY MATERIAL

C. H. FRAME AND K. L. CASCIOTTI

1. Calculating Isotopomer-Specific Ion Yields

Here we describe the results obtained from the calibration exercises recommended for calibration of isotopomer measurements using mixtures of pure isotopomer gases (ICON) and our N_2O reference gas (Westley et al., 2007). In this approach, the fragment ion yields from $^{15}N^{14}N^{16}O$ and $^{14}N^{15}N^{16}O$ are determined experimentally from analysis of these isotopomers mixed with our calibrated N_2O reference gas.

In dual inlet mode, we filled one bellows with a mixture of one of two isotopomers ($^{15}N^{14}N^{16}O$ or $^{14}N^{15}N^{16}O$) and variable proportions of our standard gas. The other bellows was filled with our standard gas. The ratios of the $\frac{^{31}NO^+}{^{30}NO^+}$ (^{31}R) and $\frac{^{45}N_2O^+}{^{44}N_2O^+}$ (^{45}R) measurements from the mixture and standard gases are graphed below as ratios ($\frac{^{31}R_{mixture}}{^{31}R_{standard}}$ and $\frac{^{45}R_{mixture}}{^{45}R_{standard}}$) in red and blue circles (Figure S.1). The raw data are given in the excel file included with the Supplementary Material.

S.1: The ratios of the ^{31}R and ^{45}R measurements from the ICON mixture and standard gases.

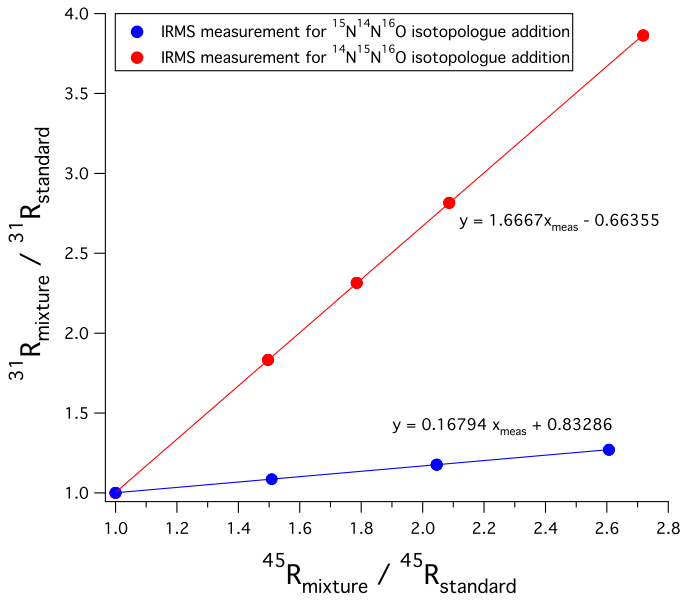

Next, we developed a series of equations that relate $\frac{^{31}\mathrm{R}_{\mathrm{mixture}}}{^{31}\mathrm{R}_{\mathrm{standard}}}$ and $\frac{^{45}\mathrm{R}_{\mathrm{mixture}}}{^{45}\mathrm{R}_{\mathrm{standard}}}$ to the yields of $^{31}NO^+$, $^{30}NO^+$, $^{45}N_2O^+$, and $^{44}N_2O^+$ from the ICON isotopologues and our standard gas. The fractional yields of the fragment ions ($^{30}NO^+$, $^{31}NO^+$) and molecular ions ($^{44}N_2O^+$, $^{45}N_2O^+$) are assumed to be constants for each of the three gases under standard operating source conditions and are defined as follows:

$$31_{\mathrm{standard}} = \frac{\text{yield } 31^+}{\text{mole standard}} \quad \text{and} \quad 31_{\mathrm{ICON}} = \frac{\text{yield } 31^+}{\text{mole ICON}}$$

$$30_{\mathrm{standard}} = \frac{\text{yield } 30^+}{\text{mole standard}} \quad \text{and} \quad 30_{\mathrm{ICON}} = \frac{\text{yield } 30^+}{\text{mole ICON}}$$

$$45_{\mathrm{standard}} = \frac{\text{yield } 45^+}{\text{mole standard}} \quad \text{and} \quad 45_{\mathrm{ICON}} = \frac{\text{yield } 45^+}{\text{mole ICON}}$$

$$44_{\mathrm{standard}} = \frac{\text{yield } 44^+}{\text{mole standard}} \quad \text{and} \quad 44_{\mathrm{ICON}} = \frac{\text{yield } 44^+}{\text{mole ICON}}$$

Then, for any mixture of ICON gas and standard gas we have:

$$^{31}\mathrm{R}_{\mathrm{mixture}} = \frac{31_{\mathrm{mixture}}}{30_{\mathrm{mixture}}} = \frac{\mathrm{F} \times \frac{\text{yield } 31^+}{\text{mole standard}} + (1-\mathrm{F}) \times \frac{\text{yield } 31^+}{\text{mole ICON}}}{\mathrm{F} \times \frac{\text{yield } 30^+}{\text{mole standard}} + (1-\mathrm{F}) \times \frac{\text{yield } 30^+}{\text{mole ICON}}}$$

and

$$^{45}\mathrm{R}_{\mathrm{mixture}} = \frac{45_{\mathrm{mixture}}}{44_{\mathrm{mixture}}} = \frac{\mathrm{F} \times \frac{\text{yield } 45^+}{\text{mole standard}} + (1-\mathrm{F}) \times \frac{\text{yield } 45^+}{\text{mole ICON}}}{\mathrm{F} \times \frac{\text{yield } 44^+}{\text{mole standard}} + (1-\mathrm{F}) \times \frac{\text{yield } 44^+}{\text{mole ICON}}}$$

where the mixing fractions F and $1 - \mathrm{F}$, are defined as follows:

$$\mathrm{F} = \frac{\text{moles standard}}{\text{moles ICON+moles standard}}$$

$$1 - \mathrm{F} = \frac{\text{moles ICON}}{\text{moles ICON+moles standard}}$$

Based on the above definitions of $^{31}\mathrm{R}_{\mathrm{mixture}}$ and $^{45}\mathrm{R}_{\mathrm{mixture}}$, if we divide $^{31}\mathrm{R}_{\mathrm{mixture}}$ by $^{31}\mathrm{R}_{\mathrm{standard}}$ or $^{45}\mathrm{R}_{\mathrm{mixture}}$ by $^{45}\mathrm{R}_{\mathrm{standard}}$ we get:

$$\frac{^{31}\mathrm{R}_{\mathrm{mixture}}}{^{31}\mathrm{R}_{\mathrm{standard}}} = \frac{\mathrm{F}+(1-\mathrm{F})\times\frac{\text{yield } 31^+}{\text{mole ICON}} \div \frac{\text{yield } 31^+}{\text{mole standard}}}{\mathrm{F}+(1-\mathrm{F})\times\frac{\text{yield } 30^+}{\text{mole ICON}} \div \frac{\text{yield } 30^+}{\text{mole standard}}}$$

$$\frac{^{45}\mathrm{R}_{\mathrm{mixture}}}{^{45}\mathrm{R}_{\mathrm{standard}}} = \frac{\mathrm{F}+(1-\mathrm{F})\times\frac{\text{yield } 45^+}{\text{mole ICON}} \div \frac{\text{yield } 45^+}{\text{mole standard}}}{\mathrm{F}+(1-\mathrm{F})\times\frac{\text{yield } 44^+}{\text{mole ICON}} \div \frac{\text{yield } 44^+}{\text{mole standard}}}$$

By making the following substitutions

$$\mathrm{A} = \frac{\text{yield } 31^+}{\text{mole ICON}} \div \frac{\text{yield } 31^+}{\text{mole standard}}$$

$$\mathrm{B} = \frac{\text{yield } 30^+}{\text{mole ICON}} \div \frac{\text{yield } 30^+}{\text{mole standard}}$$

$$\mathrm{C} = \frac{\text{yield } 45^+}{\text{mole ICON}} \div \frac{\text{yield } 45^+}{\text{mole standard}}$$

$$\mathrm{D} = \frac{\text{yield } 44^+}{\text{mole ICON}} \div \frac{\text{yield } 44^+}{\text{mole standard}}$$

we can simplify the expressions for $\frac{^{31}\mathrm{R}_{\mathrm{mixture}}}{^{31}\mathrm{R}_{\mathrm{standard}}}$ and $\frac{^{45}\mathrm{R}_{\mathrm{mixture}}}{^{45}\mathrm{R}_{\mathrm{standard}}}$:

$$\frac{^{31}\mathrm{R}_{\mathrm{mixture}}}{^{31}\mathrm{R}_{\mathrm{standard}}} = \frac{\mathrm{F}+(1-\mathrm{F})\times\mathrm{A}}{\mathrm{F}+(1-\mathrm{F})\times\mathrm{B}}$$

$$\frac{^{45}\mathrm{R}_{\mathrm{mixture}}}{^{45}\mathrm{R}_{\mathrm{standard}}} = \frac{\mathrm{F}+(1-\mathrm{F})\times\mathrm{C}}{\mathrm{F}+(1-\mathrm{F})\times\mathrm{D}}$$

Solving for F in terms of A, B, and $\frac{^{31}\mathrm{R}_{\mathrm{mixture}}}{^{31}\mathrm{R}_{\mathrm{standard}}}$ we have

$$\mathrm{F} = \frac{\mathrm{A} - \frac{^{31}\mathrm{R}_{\mathrm{mixture}}}{^{31}\mathrm{R}_{\mathrm{standard}}}\times\mathrm{B}}{\frac{^{31}\mathrm{R}_{\mathrm{mixture}}}{^{31}\mathrm{R}_{\mathrm{standard}}} - 1 + \mathrm{A} - \frac{^{31}\mathrm{R}_{\mathrm{mixture}}}{^{31}\mathrm{R}_{\mathrm{standard}}}\times\mathrm{B}}$$

By substituting this expression of F into the equation for $\frac{^{45}\mathrm{R}_{\mathrm{mixture}}}{^{45}\mathrm{R}_{\mathrm{standard}}}$ (see the column labeled 'calc ^{45}R/^{45}Rstd' in the supplementary spreadsheet), we now have an equation for $\frac{^{45}\mathrm{R}_{\mathrm{mixture}}}{^{45}\mathrm{R}_{\mathrm{standard}}}$ in terms of $\frac{^{31}\mathrm{R}_{\mathrm{mixture}}}{^{31}\mathrm{R}_{\mathrm{standard}}}$ with unknown parameters A, B, C, and D. This equation can be applied to both ^{14}N^{15}N^{16}O and ^{15}N^{14}N^{16}O ICON standard mixtures but they will have different sets of best fit values for A, B, C, and D which we call A, B, C, and D for the ^{15}N^{14}N^{16}O isotopomer and A', B', C', and D' for the ^{14}N^{15}N^{16}O isotopomer.

By definition, these parameters are all referenced to the appropriate ion yields from our reference gas, so it is possible to make direct comparisons between A and A', C and C', etc. The values of A and A' (the relative yields of $^{31}NO^+$) were fitted by varying A, B, C, and D until the calculated slopes and intercepts of the $\frac{^{45}\mathrm{R}_{\mathrm{mixture}}}{^{45}\mathrm{R}_{\mathrm{standard}}}$ vs. $\frac{^{31}\mathrm{R}_{\mathrm{mixture}}}{^{31}\mathrm{R}_{\mathrm{standard}}}$ lines aligned with those of the actual measurements from the ICON mixing analyses in Figure

S.1. The ratios calculated for $\frac{^{45}R_{mixture}}{^{45}R_{standard}}$ using the fitted values of A, B, C, D, A', B', C', and D' and the measured values of $\frac{^{31}R_{mixture}}{^{31}R_{standard}}$ are graphed below (Figure S.2). The fitted

S.2: The values of $\frac{^{45}R_{mixture}}{^{45}R_{standard}}$ calculated using fitted values (A, B, C, D and A', B', C', D') for each ion yield.

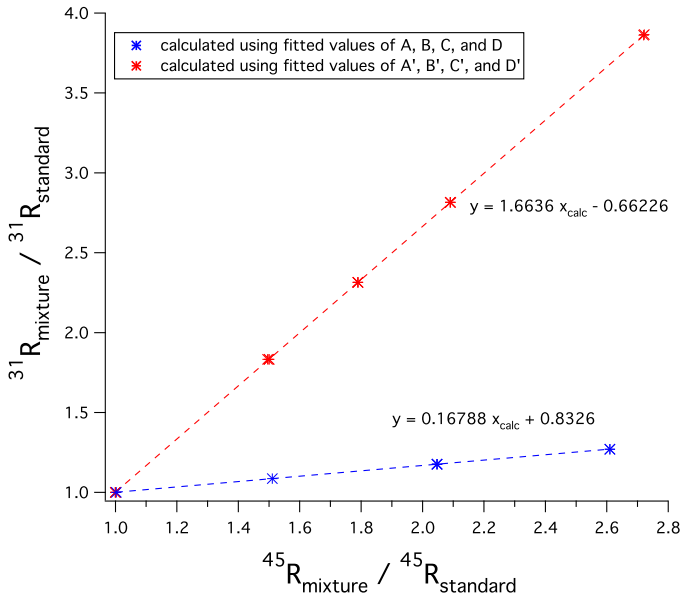

values are A = 22.65 and A' = 217. The numbers indicate that when the $^{15}N^{14}N^{16}O$ and $^{14}N^{15}N^{16}O$ isotopologues are ionized, they make 22.65 and 217 times as many $^{31}NO^+$ per mole of parent gas than the gas in our reference tank. Their ratio (= 0.104) indicates that in our ion source, the $^{14}N^{15}N^{16}O$ isotopologue yields about ten times as many $^{31}NO^+$ than the $^{15}N^{14}N^{16}O$ isotopologue.

Although the fitted values of B and B' could be used to produce a similar estimate of the $^{30}NO^+$ yields of the ICON standards referenced to our standard tank, the slopes of the calibration lines are not very sensitive to changes in B and B' because the gas in our standard tank also produces a large yield of $^{30}NO^+$.

We note that in this model of the $\frac{^{45}R_{mixture}}{^{45}R_{standard}}$ vs. $\frac{^{31}R_{mixture}}{^{31}R_{standard}}$ line, the best fit values of A and A' are dependent on the relative ion yields of $^{45}N_2O^+$ from each isotopomer (the values of the C and C' parameters). We used values of C and C' that are essentially equal to each other and very close to values that we estimated by analyzing individual ICON standard gases using a single Faraday cup and peak jumping as discussed in Westley et al (2007).

2. N_2O AND NO_2^- ACCUMULATION DURING NH_3 OXIDATION

S.3: Growth of C-113a on 50 μM NH_4^+. N_2O accumulates steadily as NH_3 is oxidized and NO_2^- accumulates. N_2O production drops off when NH_3 is completely oxidized.

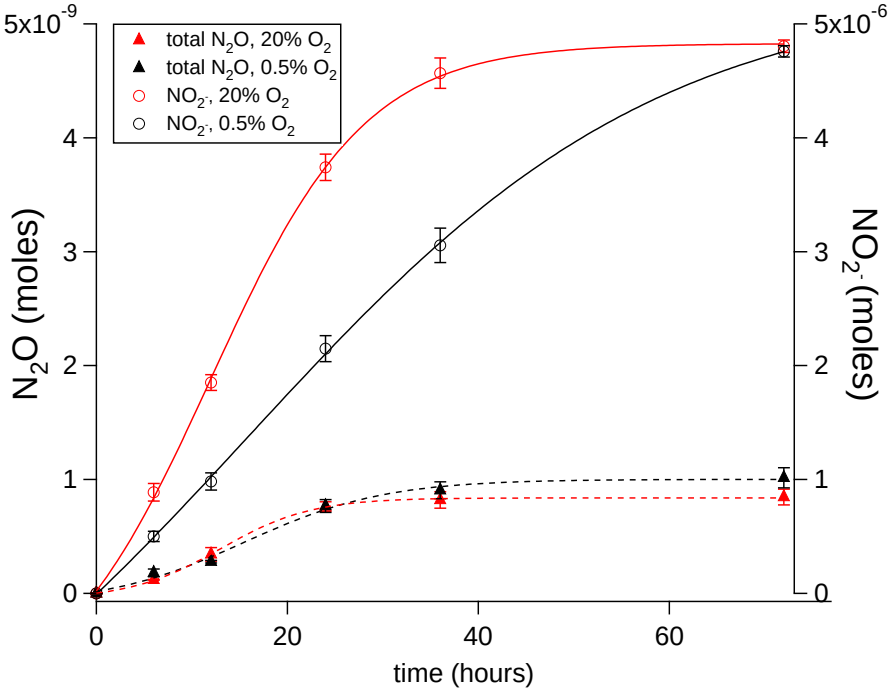

The N_2O data presented in the main text were from end-point experiments. Here we present the results of a time-course experiment used to monitor the N_2O yields over the course of an incubation. The experiment was set up and initiated in the same way as the other experiments. The initial cell density was approximately 5×10^4 cells ml^{-1}. Replicate bottles were sacrificed by adding 1 ml of 6M NaOH at different timepoints along the course of the oxidation of 50 μM NH_4^+. Total N_2O was measured for each bottle by analyzing it on the mass spectrometer with the same purge and trap system described in the main text. Yields were consistently 3×10^{-4} for bottles containing 20% O_2 and dropped from 8×10^{-4} at the 6 hour timepoint down to 4×10^{-4} at the 72 hour timepoint for bottles containing 0.5% O_2.

3. Sensitivity Analyses of Site Preference End-member values, SP_{ND} and SP_{NH2OH}, to $^{18}\epsilon_{ND}$ and $^{18}\epsilon_{NH_2OH}$

We were able to manipulate the $\delta^{18}O$ of the NO_2^- and N_2O produced during ammonia oxidation by carrying parallel experiments out in ^{18}O-enriched and unenriched water. In equation (6) (see the main text), the sensitivity of SP_{ND} and SP_{NH_2OH} to the values of the isotope effects $^{18}\epsilon_{ND}$ and $^{18}\epsilon_{NH_2OH}$ depends on the values of $\delta^{18}O\text{-}NO_2^-$, $\delta^{18}O\text{-}N_2O_{total}$, and SP_{total}. Here we demonstrate that the value of the SP_{ND} end-member may be less sensitive to $^{18}\epsilon_{ND}$ and $^{18}\epsilon_{NH_2OH}$ in ^{18}O-labeled H_2O.

To test the sensitivity of SP_{ND} to $^{18}\epsilon_{ND}$, $^{18}\epsilon_{NH_2OH}$, and SP_{NH_2OH}, values were substituted into equation (6) as follows: $SP_{total} = 17‰$, $\delta^{18}O\text{-}N_2O_{total} = 19‰$ in unlabeled water and 35‰ in labeled water, $\delta^{18}O\text{-}NO_2^- = 6‰$ in unlabeled water and 44‰ in labeled water, and $\delta^{18}O\text{-}O_2 = 25.3‰$ in all experiments. We note that these values fall within the ranges of the values of SP, $\delta^{18}O\text{-}N_2O$ (see Figure 5 in the main text), and $\delta^{18}O\text{-}NO_2^-$ that were actually observed but they are not representative of all datapoints that were included as model inputs for the non-linear regression analysis discussed in the main text. In Figures S.4A and S.4B, the best fit value of SP_{NH_2OH} (36.3‰) was used to calculate SP_{ND} and $^{18}\epsilon_{NH_2OH}$ for different $^{18}\epsilon_{ND}$. In Figures S.4C and S.4D, the best fit value of $^{18}\epsilon_{ND}$ (-8.4‰) was used to calculate SP_{ND} and $^{18}\epsilon_{NH_2OH}$ for different SP_{NH_2OH}.

Using the parameter values discussed above, SP_{ND} is more sensitive to $^{18}\epsilon_{ND}$ in unlabeled water (Figure S.4A) than in labeled water (Figure S.4B), as indicated by the larger vertical distance between contours (lines of constant $^{18}\epsilon_{ND}$) in S.4A than in S.4B. SP_{ND} is also more sensitive to $^{18}\epsilon_{NH_2OH}$ in unlabeled water (Figures S.4A and S.4C) than labeled water (Figures S.4B and S.4D). This is evident in that the lines of constant $^{18}\epsilon_{ND}$ or SP_{NH_2OH} are more horizontal in S.4B and S.4D than they are in S.4A or S.4C.

We also see this in Supplementary Tables 1 and 2, where we have recalculated SP_{ND} using values of $^{18}\epsilon_{NH_2OH}$, $^{18}\epsilon_{ND}$, and SP_{NH_2OH} that are one standard deviation higher or lower than the best fit values. For the same set of best fit values and standard deviations, the calculated range of SP_{ND} values is larger in unlabeled water (Supplementary Table 1) than in labeled water (Supplementary Table 2).

This data set had a larger range of $\delta^{18}O\text{-}N_2O$ values than it would have had if we had only included data from cultures in unlabeled water. The larger range of $\delta^{18}O\text{-}N_2O$ in labeled water helps explain the reduced sensitivity of the model parameters to each other in labeled water. Future experiments may expand this range even further by increasing the difference between the substrate $\delta^{18}O\text{-}O_2$ and $\delta^{18}O\text{-}H_2O$ values.

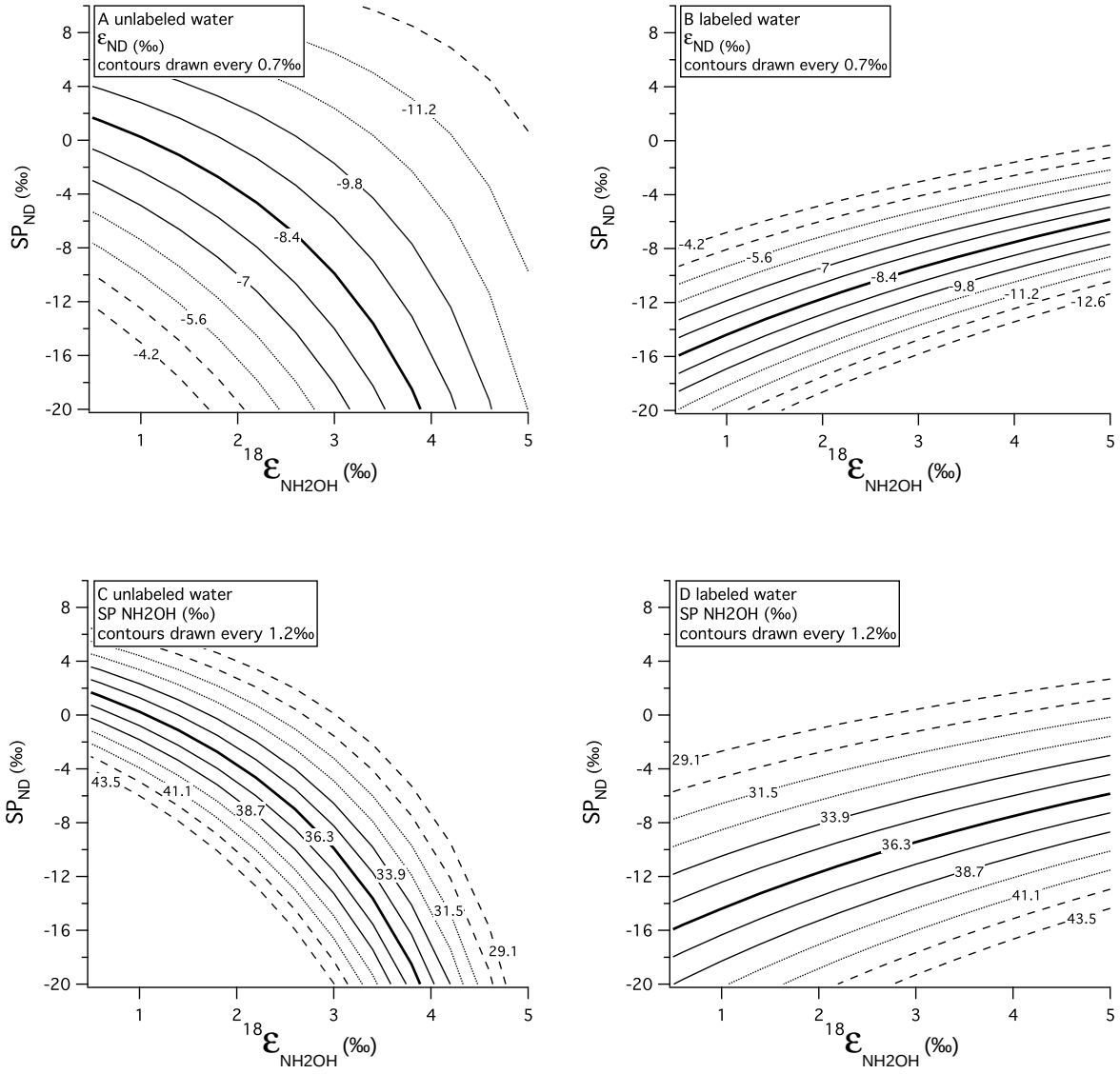

S.4: Sensitivity of SP_{ND} estimates from the end-member mixing model to variations in $^{18}\epsilon_{NH_2OH}$ for different values of $^{18}\epsilon_{ND}$ (contours in panels A and B) or SP_{NH_2OH} (contours in panels C and D), in water labeled with ^{18}O (panels B and D) and in unlabeled water (panels A and C). In all plots, lines were drawn every $\sigma/2$ (based on the estimated standard deviations in Table 1 of the main text) for the contoured variable.

TABLE 1. The effect of uncertainty in $^{18}\epsilon_{NH_2OH}$, $^{18}\epsilon_{ND}$, and SP_{NH_2OH} on the calculated value of SP_{ND} in unlabeled water ($\delta^{18}O \simeq$ -5‰). All entries are in ‰. Bold entries in the first three columns have been changed ± one standard deviation above and below the best fit values.

$^{18}\epsilon_{NH_2OH}$	$^{18}\epsilon_{ND}$	SP_{NH_2OH}	SP_{ND}	SP_{total}	$\delta^{18}O$-N_2O_{total}	$\delta^{18}O$-NO_2-	$\delta^{18}O$-O_2
2.1	-8.4	36.3	**-4.1**	17	19	6	25.3
2.9	-8.4	36.3	**-9.1**	17	19	6	25.3
3.7	-8.4	36.3	**-17.2**	17	19	6	25.3
2.9	**-9.8**	36.3	**-1.2**	17	19	6	25.3
2.9	**-8.4**	36.3	**-9.1**	17	19	6	25.3
2.9	**-7.0**	36.3	**-17.1**	17	19	6	25.3
2.9	-8.4	**33.9**	**-5.9**	17	19	6	25.3
2.9	-8.4	**36.3**	**-9.1**	17	19	6	25.3
2.9	-8.4	**38.7**	**-12.4**	17	19	6	25.3

TABLE 2. The effect of uncertainty in $^{18}\epsilon_{NH_2OH}$, $^{18}\epsilon_{ND}$, and SP_{NH_2OH} on the calculated value of SP_{ND} in ^{18}O-labeled water ($\delta^{18}O \simeq 40$‰). All entries are in ‰. Bold entries in the first three columns have been changed ± one standard deviation above and below the best fit values.

$^{18}\epsilon_{NH_2OH}$	$^{18}\epsilon_{ND}$	SP_{NH_2OH}	SP_{ND}	SP_{total}	$\delta^{18}O$-N_2O_{total}	$\delta^{18}O$-NO_2-	$\delta^{18}O$-O_2
2.1	-8.4	36.3	**-11.5**	17	35	44	25.3
2.9	-8.4	36.3	**-9.7**	17	35	44	25.3
3.7	-8.4	36.3	**-8.1**	17	35	44	25.3
2.9	**-9.8**	36.3	**-11.8**	17	35	44	25.3
2.9	**-8.4**	36.3	**-9.7**	17	35	44	25.3
2.9	**-7**	36.3	**-7.5**	17	35	44	25.3
2.9	-8.4	**33.9**	**-6.3**	17	35	44	25.3
2.9	-8.4	**36.3**	**-9.7**	17	35	44	25.3
2.9	-8.4	**38.7**	**-13.0**	17	35	44	25.3